








**Strain relaxation induced transverse resistivity anomalies in SrRuO<sub>3</sub> thin films**

Ludi Miao <sup>1</sup>, Nathaniel J. Schreiber,<sup>2</sup> Hari P. Nair,<sup>2</sup> Berit H. Goodge <sup>3</sup>, Shengwei Jiang <sup>3</sup>, Jacob P. Ruf <sup>1</sup>, Yonghun Lee,<sup>3</sup> Matthew Fu <sup>3</sup>, Boris Tsang <sup>1</sup>, Yingfei Li,<sup>2</sup> Cyrus Zeledon,<sup>2</sup> Jie Shan,<sup>1,3,4</sup> Kin Fai Mak,<sup>1,3,4</sup> Lena F. Kourkoutis <sup>3,4</sup>, Darrell G. Schlom,<sup>2,4</sup> and Kyle M. Shen<sup>1,4,\*</sup>

<sup>1</sup>*Department of Physics, Laboratory of Atomic and Solid State Physics, Cornell University, Ithaca, New York 14853, USA*

<sup>2</sup>*Department of Materials Science and Engineering, Cornell University, Ithaca, New York 14853, USA*

<sup>3</sup>*School of Applied and Engineering Physics, Cornell University, Ithaca, New York 14853, USA*

<sup>4</sup>*Kavli Institute at Cornell for Nanoscale Science, Ithaca, New York 14853, USA*



(Received 27 April 2020; accepted 8 July 2020; published 7 August 2020)

Here, we report a magnetotransport study of high-quality SrRuO<sub>3</sub> thin films with high residual resistivity ratios grown by reactive oxide molecular-beam epitaxy. The transverse resistivity exhibits clear anomalies which are typically believed to be signatures of the topological Hall effect and the presence of magnetic skyrmions. By systematically investigating these anomalies as a function of temperature, field, film thickness, and excitation currents we verify that these anomalies originate from a two-channel anomalous Hall effect arising from magnetic inhomogeneities in the samples and not from an intrinsic topological Hall effect. Using a combination of magnetic circular dichroism, scanning transmission electron microscopy, x-ray diffraction, and magnetotransport, we discover that strain relaxation effects in the films are the origin of these inhomogeneities. Our results shed light on the recently reported Hall effect anomalies in SrRuO<sub>3</sub> thin films and heterostructures and provide an approach to determine whether such anomalies arise from an intrinsic topological Hall effect or from extrinsic mechanisms.

DOI: [10.1103/PhysRevB.102.064406](https://doi.org/10.1103/PhysRevB.102.064406)

**I. INTRODUCTION**

The Hall effect, in its various forms, has long been a central topic in condensed-matter physics, including the quantum Hall effect [1], quantum spin Hall effect [2], and anomalous Hall effect [3]. Recently, the topological Hall effect, characterized by an anomaly in the transverse resistivity, has attracted great interest for its potential sensitivity to the topological charge of a magnetic system, such as magnetic skyrmions [4], which can be otherwise challenging to detect using other probes. Possible signatures of the topological Hall effect were recently reported in SrRuO<sub>3</sub> thin films and heterostructures [5–8], where it was believed that the Dzyaloshinskii-Moriya interaction at the interfaces could give rise to magnetic skyrmions [5,6]. It has, however, also been proposed that the anomalies in  $\rho_{xy}$  could also be produced in magnetically inhomogeneous systems, where different regions produce different anomalous Hall signals which, when combined, can closely mimic the signatures of the topological Hall effect [9–14]. In SrRuO<sub>3</sub> thin films and heterostructures, however, it can be challenging to distinguish between these possible origins of these anomalies in the transverse resistivity.

Here, we show that even in very high quality SrRuO<sub>3</sub> films grown by molecular-beam epitaxy with thicknesses in the range of tens of nanometers, magnetic domains and inhomogeneities can, nonetheless, give rise to extrinsic anomalies in  $\rho_{xy}$  that could otherwise be interpreted as a signature of the topological Hall effect. Using a combination of

magnetotransport, magneto-optical measurements, scanning transmission electron microscopy, and x-ray diffraction measurements, we find that anomalies in the transverse resistivities can instead be associated with magnetic inhomogeneities likely associated with strain relaxation. The insensitivity of these anomalies to both canted magnetic fields and large electrical currents suggests that spatial inhomogeneities, and not the formation of magnetic skyrmions, are the most likely origin of the observed effects. These results not only provide important insights into the physics of SrRuO<sub>3</sub> thin films and heterostructures but also describe approaches to determine whether anomalies in  $\rho_{xy}$  are extrinsic or arise from an intrinsic topological Hall effect.

**II. EXPERIMENT**

SrRuO<sub>3</sub> thin films were synthesized on (110) NdGaO<sub>3</sub> substrates by reactive oxide molecular-beam epitaxy in an absorption-controlled regime, which reduces the number of defects related to cation nonstoichiometry, as detailed in [15]. The compressive strain imposed by the (110) NdGaO<sub>3</sub> substrate is  $-1.77\%$  along the [001] direction and  $-1.58\%$  along the  $[\bar{1}10]$  direction. The SrRuO<sub>3</sub> films were grown at a substrate temperature of 650 °C and a background oxidant partial pressure of  $10^{-6}$  Torr of distilled ozone ( $\sim 80\% \text{O}_3 + 20\% \text{O}_2$ ). The low amount of disorder in the films is evident from their low residual resistivities ( $\rho_{4K} \sim 10 \mu\Omega \text{ cm}$ ), which are substantially (i.e.,  $\sim 4\text{--}5$  times) lower than SrRuO<sub>3</sub> thin films grown by other techniques such as pulsed laser deposition [7,9].

The phase purity and structural perfection of the samples were characterized using a laboratory-based x-ray

\*kmshen@cornell.edu

diffractometer (XRD) with Cu  $K\alpha$  radiation (Rigaku Smart-Lab and Malvern Panalytical Empyrean diffractometers). A subset of films was also imaged using cross-sectional transmission electron microscopy, lamellae of which were prepared using the standard focused ion beam lift-out process. High-angle annular dark-field scanning transmission electron microscopy (HAADF-STEM) images were acquired on an aberration-corrected FEI Titan Themis at 300 keV. Films were patterned into Hall bars for longitudinal and transverse resistivity measurements, and the magnetism of a subset of the films was examined using magnetic circular dichroism (MCD) using the setup shown in Fig. 1(a).

### III. RESULTS AND DISCUSSION

In Fig. 1(b), we show the longitudinal resistivity as a function of temperature  $\rho_{xx}(T)$  of a 30-nm-thick SrRuO<sub>3</sub> film measured in zero magnetic field.  $\rho_{xx}(T)$  shows a characteristic kink at the ferromagnetic Curie temperature,  $T_C = 158$  K, and has a residual resistivity ratio  $\rho(300\text{ K})/\rho(4\text{ K}) = 21.4$ , demonstrating the high crystalline quality and low amounts of disorder in the sample. The hysteretic behavior of the resistivity and the MCD signal in magnetic fields as shown in Figs. 1(c) and 1(d) confirm the ferromagnetic behavior. In Fig. 1(d), we show the transverse resistivity  $\rho_{xy}$  as a function of the out-of-plane magnetic field  $\mu_0 H$  at 130 K, which clearly shows two pronounced peaks around  $\pm 0.12$  T, the typical signature of the topological Hall effect.

To more systematically investigate the origin of the anomaly in  $\rho_{xy}$ , we investigated a series of samples as a function of both thickness and temperature, as shown in Fig. 2(a). Samples with thicknesses between 20 and 40 nm show obvious anomalies in  $\rho_{xy}$ , whereas samples no thicker than 15 nm do not clearly exhibit such behavior, nor do substantially thicker samples (i.e., 60 nm). In Fig. 2(b), we summarize the amplitude of the anomaly in  $\rho_{xy}$  as defined in Fig. 2(a), showing that these anomalies are most prominent within a narrow temperature range of  $120\text{ K} < T < T_C$  and a film thickness range of 20 to 40 nm. This temperature window follows the sign-switching temperatures of the anomalous Hall effects, which is consistent with previous reports in other SrRuO<sub>3</sub> systems [9,16,17] and implies that the origin of  $\rho_{\text{anomaly}}$  likely arises from the combination of anomalous Hall effects from two channels.

In order to determine the mechanism of this anomaly, we investigated the dependence of  $\rho_{\text{anomaly}}$  on the current density, the canting angle of the magnetic field, and the so-called minor loop. The dependence of  $\rho_{\text{anomaly}}$  on the current is shown in Figs. 3(a) and 3(b) and clearly shows no obvious dependence over a change in the current density of over two orders of magnitude up to  $10^5\text{ A cm}^{-2}$ . In Figs. 3(c) and 3(d), we show the dependence of  $\rho_{\text{anomaly}}$  on field canting angles  $\theta_{\text{tilt}}$ , which again show no dependence on canting angles  $\theta_{\text{tilt}}$  up to  $60^\circ$ . Finally, the dependence of  $\rho_{\text{anomaly}}$  on the minor loop is shown in Figs. 3(e) and 3(f), where a closed-loop field sweep is applied, which has a different minimum field value  $\mu_0 H_{\text{min}}$  and the same maximum field value  $\mu_0 H_{\text{max}}$ . In this case, we find that  $\rho_{\text{anomaly}}$  systematically decreases as  $\mu_0 H_{\text{min}}$  increases. In systems which exhibit magnetic skyrmions,

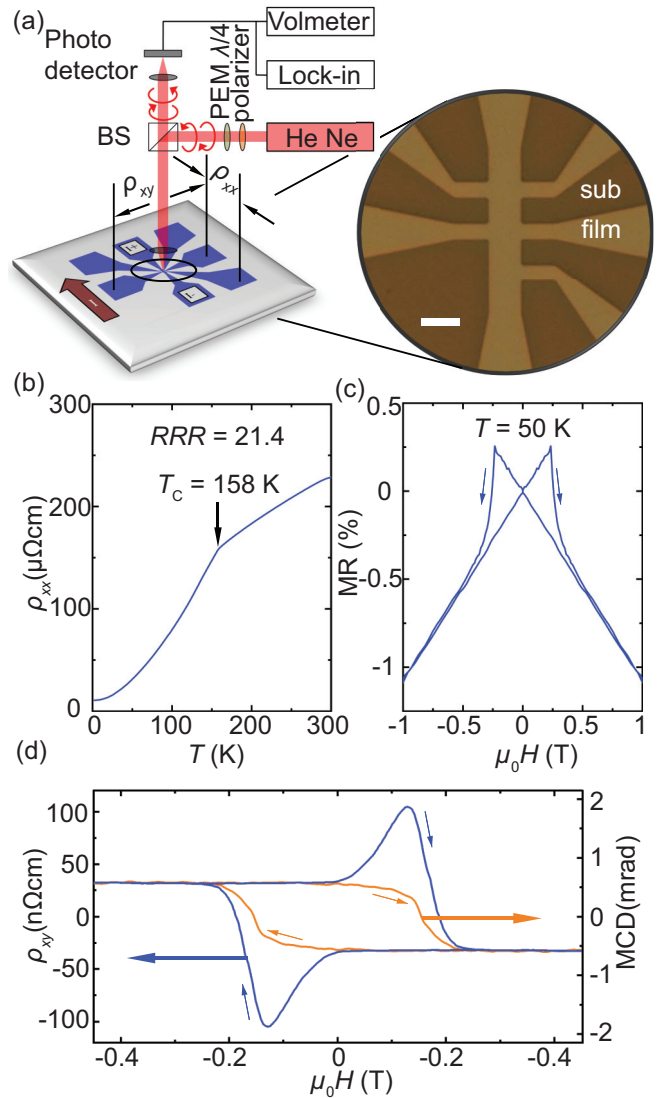


FIG. 1. (a) Illustration of the MCD measurement setup, where the He Ne laser with  $\lambda = 633$  nm, the beam splitter, the lock-in amplifier, and the photoelastic modulator are labeled by He Ne, BS, lock-in, and PEM, respectively. The lock-in amplifiers are set at the same frequency as the PEM. The inset is the optical image of a 30-nm-thick SrRuO<sub>3</sub>/NdGaO<sub>3</sub> Hall bar device. The length of the scale bar is  $20\ \mu\text{m}$ . (b) In-plane resistivity  $\rho_{xx}$  as a function of the temperature  $T$  of the film. (c) Magnetoresistance MR defined as  $[\rho_{xx}(\mu_0 H) - \rho_{xx}(0)]/\rho_{xx}(0)$  as a function of the out-of-plane magnetic field  $\mu_0 H$  showing FM hysteretic behaviors, measured at  $T = 50$  K. The longitudinal resistivity was symmetrized about the magnetic fields to take out the minor transverse resistivity components. (d) MCD signal  $\Delta A$  and transverse resistivity  $\rho_{xy}$  as a function of out-of-plane magnetic field  $\mu_0 H$ , measured at 130 K. The field sweeping directions are marked by arrows. Both the longitudinal resistivity and the MCD signal were antisymmetrized about the magnetic fields and then subtracted by a linear background so that they are flat at the high fields.

$\rho_{\text{anomaly}}$  should be strongly dependent on the current density since skyrmions are mobile and can be driven by electrical currents, which leads to a time-dependent term of the fictitious field and subsequent suppression of the topological Hall effect

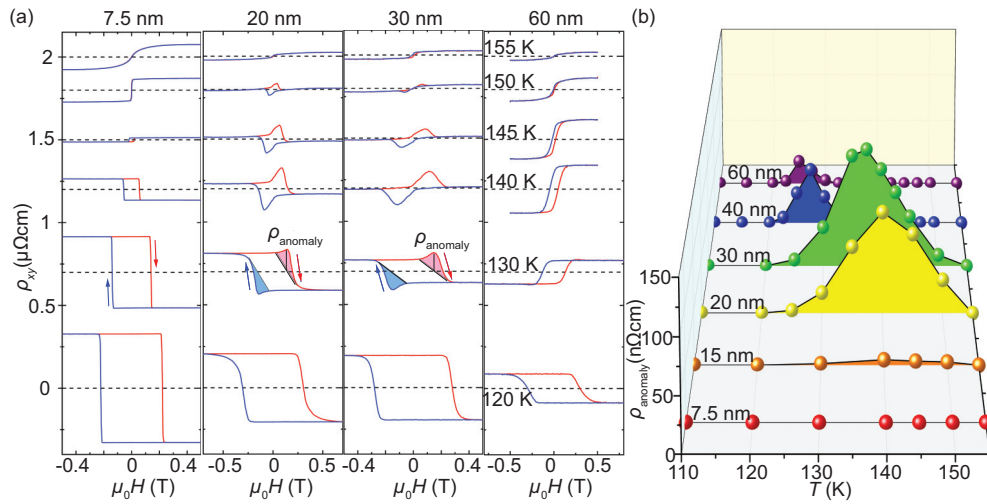


FIG. 2. (a) Transverse resistivity  $\rho_{xy}$  as a function of out-of-plane magnetic field  $\mu_0 H$  of SrRuO<sub>3</sub>/NdGaO<sub>3</sub> Hall bars with various SrRuO<sub>3</sub> thicknesses, measured at different temperatures. The transverse resistivity anomalies  $\rho_{\text{anomaly}}$  are labeled. The field sweeping directions are marked by arrows. (b) A summary of the transverse resistivity anomalies  $\rho_{\text{anomaly}}$  as a function of temperature for SrRuO<sub>3</sub>/NdGaO<sub>3</sub> Hall bars with various SrRuO<sub>3</sub> thicknesses.

[18], as observed in MnSi nanowires, where a current density of  $<10^4 \text{ A cm}^{-2}$  will start to suppress any observed effects. Furthermore, it has been reported that the skyrmion textures can easily be disrupted by a canted magnetic field, as reported in EuO, where the topological Hall effect can be completely suppressed by canting angles as small as  $4^\circ$  [19]. Finally, Kan *et al.* [9] and Groenendijk *et al.* [10] argued that a decrease in  $\rho_{\text{anomaly}}$  as a function of  $\mu_0 H_{\text{min}}$  indicates the hysteretic behavior of  $\rho_{\text{anomaly}}$ , which is not in line with skyrmion formation, but rather the ferromagnetic state itself. Therefore, none of these aforementioned measurements appear to be consistent

with an interpretation where  $\rho_{\text{anomaly}}$  arises from the formation of magnetic skyrmions.

Having ruled out magnetic skyrmions and the topological Hall effect as the origin of these observed behaviors, we then investigated the possibility of magnetic inhomogeneities which could give rise to  $\rho_{\text{anomaly}}$ , as proposed by Kan *et al.* [9]. In this scenario, different regions of the sample produce differing anomalous Hall effects (i.e., a two-channel anomalous Hall effect) which subsequently give rise to the observed  $\rho_{\text{anomaly}}$ . To investigate this possibility, we performed HAADF-STEM measurements of a thin (7.5 nm) sample

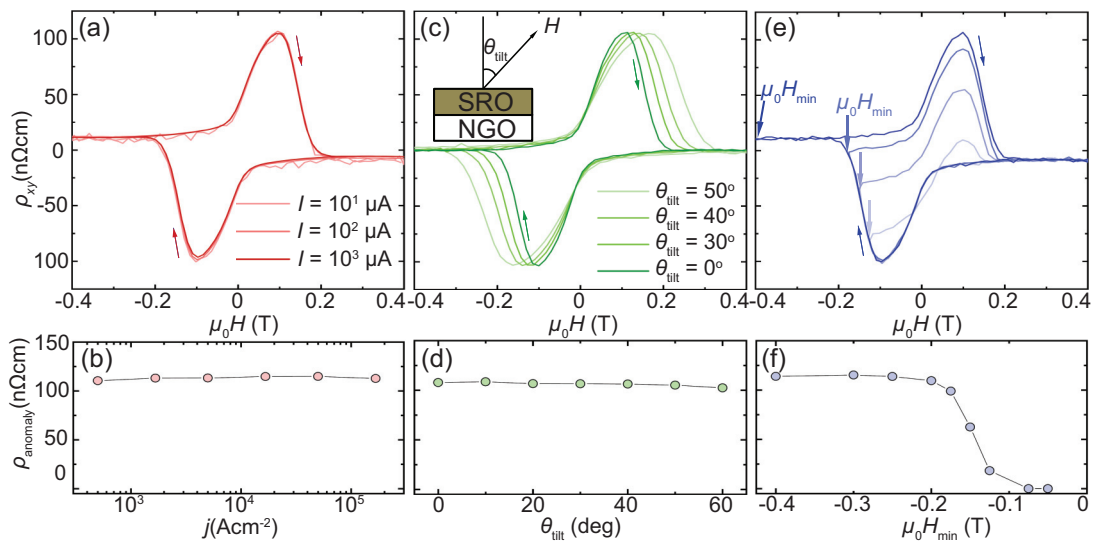


FIG. 3. (a)  $\rho_{xy}$  as a function of the magnetic field, measured with various excitation currents, on a 30-nm-thick sample. (b)  $\rho_{\text{anomaly}}$  as a function of the excitation current density  $j$ , showing the robustness of the resistivity anomalies against the excitation current densities. (c)  $\rho_{xy}$  as a function of magnetic field, measured with various field canting angles  $\theta_{\text{tilt}}$  from the surface normal direction. (d)  $\rho_{\text{anomaly}}$  as a function of  $\theta_{\text{tilt}}$ , showing the robustness of the resistivity anomalies against the canting fields. (e) Minor loops of the transverse resistivity  $\rho_{xy}$ , measured with various magnetic field end points  $\mu_0 H_{\text{min}}$ . (f) Transverse resistivity anomalies  $\rho_{\text{anomaly}}$  as a function of  $\mu_0 H_{\text{min}}$ . All of the above results were measured at  $T = 140 \text{ K}$ , where  $\rho_{\text{anomaly}}$  is nearly at the maximum. The field sweeping directions are marked by arrows.



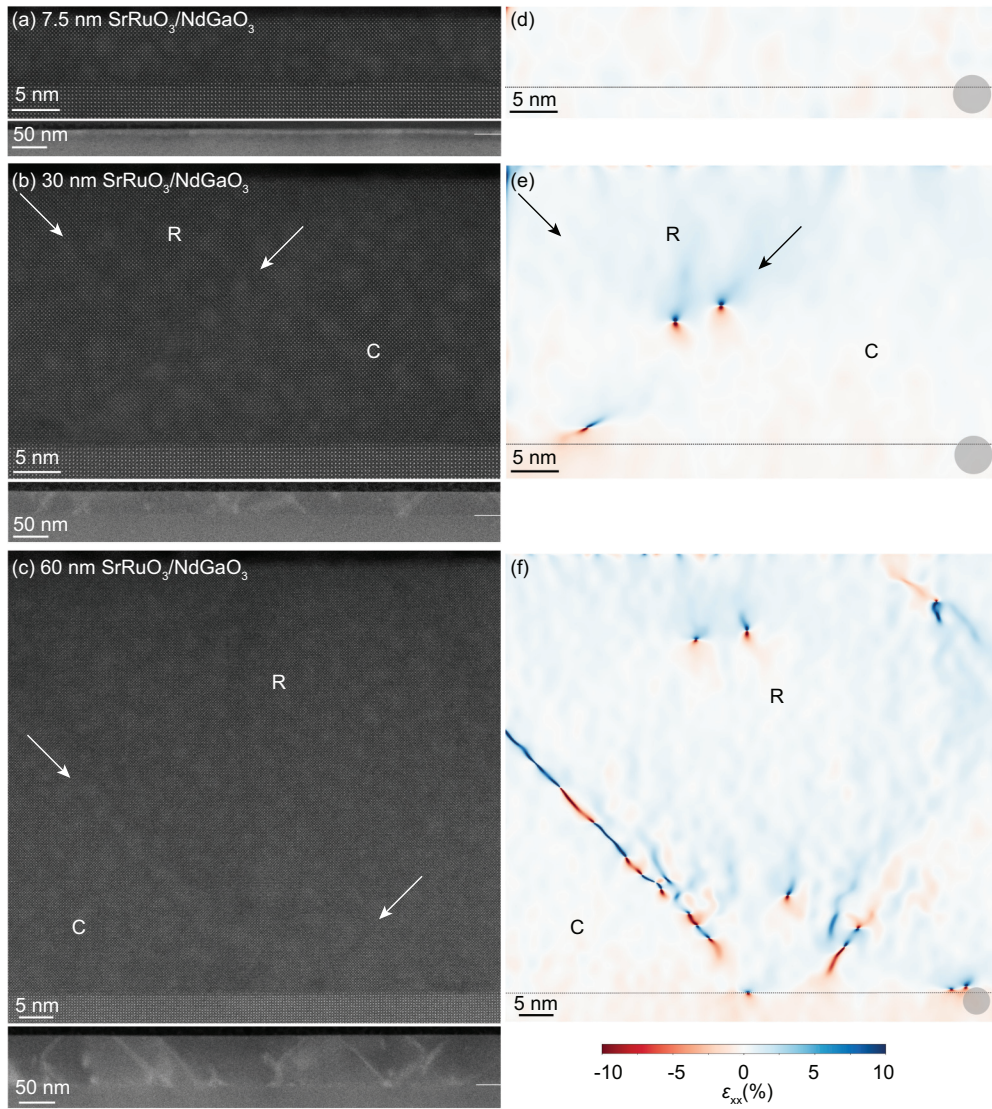


FIG. 4. HAADF-STEM high-magnification images (top) and representative medium-angle annular dark-field STEM images (bottom) over larger-size fields of view of (a) 7.5-nm, (b) 30-nm, and (c) 60-nm thick films, projected along the [100] pseudocubic direction. The dislocation regions in (b) and (c) are highlighted by white arrows. (d)–(f) The respective in-plane components of the strain tensor ( $\epsilon_{xx}$  color scales) obtained from the STEM images by phase lock-in analysis. The circles show the 4-nm real-space resolution of the phase lock-in analysis. Regions above the crystalline dislocation boundaries (away from the interface) show larger strain amplitudes, while regions below the boundaries (closer to the interface) show smaller local strain amplitudes. We therefore assign the designations “relaxed” (R) and “coherent” (C) to these regions, respectively.

which does not exhibit any  $\rho_{\text{anomaly}}$ , a 30-nm-thick sample where  $\rho_{\text{anomaly}}$  is maximum, and a much thicker 60-nm film, as shown in Figs. 4(a), 4(b), and 4(c). While the thinner sample exhibits a highly coherent crystalline structure with no obvious defect structure, the thicker films clearly exhibit dislocations along the [011] pseudocubic direction, as indicated by white arrows in Figs. 4(b) and 4(c), presumably due to lattice relaxation. The local in-plane strain  $\epsilon_{xx}$  was mapped by phase lock-in analysis [20–23] to track spatial variations in each film, as shown in Figs. 4(d), 4(e), and 4(f). The 7.5-nm-thick sample displays a relatively homogeneous coherent local strain with  $\epsilon_{xx} \sim 0$  throughout the whole film. In contrast, the 30-nm-thick sample starts to show signatures of strain relaxation. The sample displays two types of distinct regions: one type (labeled by “C”) remains coherently strained with  $\epsilon_{xx}$

close to zero, and the other type (labeled by “R”) has relaxed strain with  $\epsilon_{xx} \sim 0.5\%$ . The C region is located close to the interface, whereas the R region is located close to the surface. These two regions are separated by dislocations lines that are along the [011] pseudocubic direction. Given that in SrRuO<sub>3</sub> films, the anomalous Hall effect sign and amplitude, magnetic anisotropy, and  $T_C$  all depend on the strain, these regions are the likely origin of inhomogeneous magnetic domains, thereby giving rise to a two-channel anomalous Hall effect. The 60-nm-thick sample displays a morphology similar to that of the 30-nm-thick film, but with larger fractions of the R region, stronger dislocations lines, and strain variations in the R region and along the dislocations lines. In this case, this film cannot be simply described by a two-channel model but should be governed by a more complicated multichannel

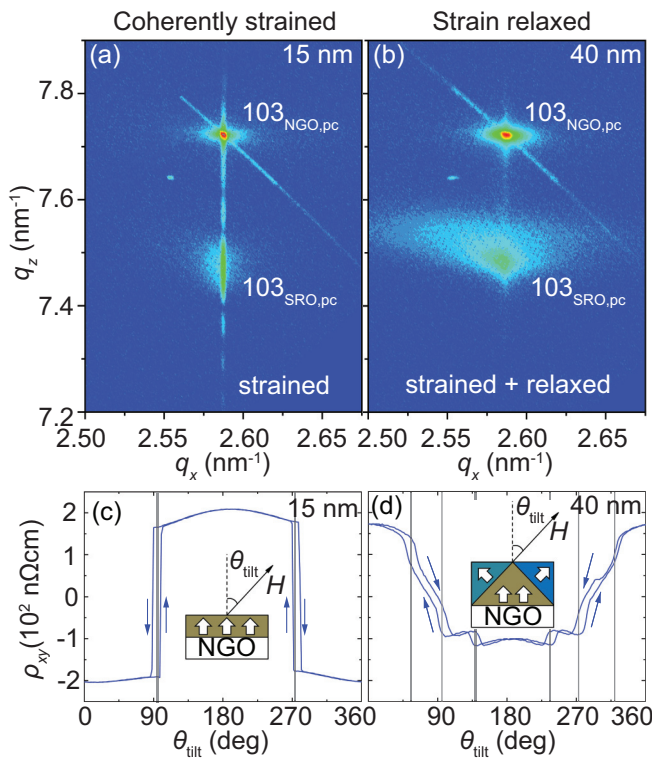


FIG. 5. (a) and (b) XRD reciprocal space maps of a 15-nm-thick film and a 40-nm-thick film, respectively, around the SrRuO<sub>3</sub> (SRO) 103 and NdGaO<sub>3</sub> (NGO) 103 pseudocubic (pc) reflection peaks. (c) and (d) Transverse resistivity  $\rho_{xy}$  as a function of field canting angles  $\theta_{\text{tilt}}$  of a 15-nm-thick film and a 40-nm-thick SRO film, respectively, measured at 140 K, showing a single magnetic domain for the 15-nm-thick sample and multiple magnetic domains for the 40-nm-thick sample. The angle sweeping directions are marked by arrows.

model, which leads to a nonzero but smaller  $\rho_{\text{anomaly}}$ , as shown in Fig. 2. Figures 5(a) and 5(b) show the XRD reciprocal map of a 15-nm-thick film and a 40-nm-thick film, revealing a coherent strain in the former one and a strain relaxation in the latter one, which are likewise consistent with this picture.

To verify this picture of magnetic inhomogeneity in strain-relaxed films, we measured  $\rho_{xy}$  as a function of the magnetic field canting angle  $\theta_{\text{tilt}}$  in the 15- and 40-nm-thick films in which the reciprocal space maps were measured in Figs. 5(a) and 5(b). The results are shown in Figs. 5(c) and 5(d), where  $\rho_{xy}$  should show switching behavior around the magnetic hard axes. Such behavior is indeed observed in the 15-nm-thick sample [Fig. 5(c)], which exhibits two sharp transitions around  $\theta_{\text{tilt}} = 90^\circ$  and  $270^\circ$ , indicating that the film is composed of a single magnetic domain with easy axes along the out-of-plane direction. In contrast, the 40-nm-thick

film in Fig. 5(d) displays four additional transitions, roughly separated from the original transitions by  $45^\circ$ , indicating that this film contains additional magnetic domains with easy axes canted  $45^\circ$  from the out-of-plane direction, presumably related to the strain-relaxed regions observed in Fig. 4. Such an easy-axis canting can be understood in terms of a possible Ru-O-Ru bond angle and bond length change as a result of the strain relaxation. These results verify that the transverse resistivity anomalies observed in these SrRuO<sub>3</sub> films indeed result from the correlated structural and magnetic inhomogeneities in our films, as proposed by Kan *et al.* [9]. We note that although our thicker films exhibit strain relaxation, they nevertheless exhibit relatively low amounts of disorder, as determined by their low residual resistivities, compared to the majority of SrRuO<sub>3</sub> films in the literature, indicating that relatively subtle effects can, nevertheless, give rise to a spurious indication of the topological Hall effect.

By performing a systematic investigation of SrRuO<sub>3</sub> films as a function of thickness and temperature and combining a variety of experimental probes, including magnetic circular dichroism, magnetotransport, transmission electron microscopy, and x-ray diffraction, we can conclude that  $\rho_{\text{anomaly}}$  observed in our SrRuO<sub>3</sub> films do not arise from the formation of magnetic skyrmions, but rather from the formation of structural and magnetic domains arising from strain relaxation, which gives rise to a two-channel anomalous Hall effect which mimics an intrinsic topological Hall effect. By providing not only a solid example verifying the magnetic inhomogeneity explanation but also a microscopic picture revealing the origin of the magnetic inhomogeneities, our results shed light on the recently reported Hall effect anomalies in SrRuO<sub>3</sub> films.

All relevant data are available from the authors upon reasonable request.

#### ACKNOWLEDGMENTS

This work was supported by the National Science Foundation [Platform for the Accelerated Realization, Analysis, and Discovery of Interface Materials (PARADIM)] under Cooperative Agreement No. DMR-1539918, NSF Grant No. DMR-1709255, Air Force Office of Scientific Research Grant No. FA9550-15-1-0474, the Department of Energy (Award No. DE-SC0019414), and the Gordon and Betty Moore Foundation's EPiQS Initiative through Grant No. GBMF3850 to Cornell University. This work made use of the Cornell Center for Materials Research (CCMR) Shared Facilities, which are supported through the NSF MRSEC Program (Grant No. DMR-1719875). Device fabrication and substrate preparation were performed in part at the Cornell NanoScale Facility, a member of the National Nanotechnology Coordinated Infrastructure (NNCI), which is supported by the NSF (Grant No. NNCI-1542081).

- [1] D. R. Yennie, *Rev. Mod. Phys.* **59**, 781 (1987).
- [2] M. Z. Hasan and C. L. Kane, *Rev. Mod. Phys.* **82**, 3045 (2010).
- [3] D. Xiao, M.-C. Chang, and Q. Niu, *Rev. Mod. Phys.* **82**, 1959 (2010).

- [4] A. Fert, N. Reyren, and V. Cros, *Nat. Rev. Mater.* **2**, 17031 (2017).
- [5] J. Matsuno, N. Ogawa, K. Yasuda, F. Kagawa, W. Koshibae, N. Nagaosa, Y. Tokura, and M. Kawasaki, *Sci. Adv.* **2**, e1600304 (2016).

- [6] Y. Ohuchi, J. Matsuno, N. Ogawa, Y. Kozuka, M. Uchida, Y. Tokura, and M. Kawasaki, *Nat. Commun.* **9**, 213 (2018).
- [7] L. Wang, Q. Feng, Y. Kim, R. Kim, K. H. Lee, S. D. Pollard, Y. J. Shin, H. Zhou, W. Peng, D. Lee, W. Meng, H. Yang, J. H. Han, M. Kim, Q. Lu, and T. W. Noh, *Nat. Mater.* **17**, 1087 (2018).
- [8] W. Wang, M. W. Daniels, Z. Liao, Y. Zhao, J. Wang, G. Koster, G. Rijnders, C.-Z. Chang, D. Xiao, and W. Wu, *Nat. Mater.* **18**, 1054 (2019).
- [9] D. Kan, T. Moriyama, K. Kobayashi, and Y. Shimakawa, *Phys. Rev. B* **98**, 180408(R) (2018).
- [10] D. J. Groenendijk, C. Autieri, T. C. van Thiel, W. Brzezicki, N. Gauquelin, P. Barone, K. H. W. van den Bos, S. van Aert, J. Verbeeck, A. Filippetti, S. Picozzi, M. Cuoco, and A. D. Caviglia, *Phys. Rev. Research* **2**, 023404 (2020).
- [11] D. Kan and Y. Shimakawa, *Phys. Status Solidi B* **255**, 1800175 (2018).
- [12] G. Malsch, D. Ivaneyko, P. Milde, L. Wysocki, L. Yang, P. H. M. van Loosdrecht, I. Lindfors-Vrejoiu, and L. M. Eng, *ACS Appl. Nano Mater.* **3**, 1182 (2020).
- [13] L. Wysocki, J. Schöpf, M. Ziese, L. Yang, A. Kovács, L. Jin, R. B. Versteeg, A. Bliesener, F. Gunkel, L. Kornblum, R. Dittmann, P. H. M. van Loosdrecht, and I. Lindfors-Vrejoiu, *ACS Omega* **5**, 5824 (2020).
- [14] D. Kan, K. Kobayashi, and Y. Shimakawa, *Phys. Rev. B* **101**, 144405 (2020).
- [15] H. P. Nair, J. P. Ruf, N. J. Schreiber, L. Miao, M. L. Grandon, D. J. Baek, B. H. Goodge, J. P. C. Ruff, L. F. Kourkoutis, K. M. Shen, and D. G. Schlom, *APL Mater.* **6**, 101108 (2018).
- [16] Q. Qin, L. Liu, W. Lin, X. Shu, Q. Xie, Z. Lim, C. Li, S. He, G. M. Chow, and J. Chen, *Adv. Mater.* **31**, 1807008 (2019).
- [17] H. Wang, Y. Dai, Z. Liu, Q. Xie, C. Liu, W. Lin, L. Liu, P. Yang, J. Wang, T. V. Venkatesan, G. M. Chow, H. Tian, Z. Zhang, and J. Chen, *Adv. Mater.* **32**, 1904415 (2020).
- [18] D. Liang, J. P. DeGrave, M. J. Stolt, Y. Tokura, and S. Jin, *Nat. Commun.* **6**, 8217 (2015).
- [19] M. F. Gely, A. Parra-Rodriguez, D. Bothner, Y. M. Blanter, S. J. Bosman, E. Solano, and G. A. Steele, *Phys. Rev. B* **95**, 245115 (2017).
- [20] B. H. Savitzky, I. El Baggari, A. S. Admasu, J. Kim, S.-W. Cheong, R. Hovden, and L. F. Kourkoutis, *Nat. Commun.* **8**, 1883 (2017).
- [21] M. J. Lawler, K. Fujita, J. Lee, A. R. Schmidt, Y. Kohsaka, C. K. Kim, H. Eisaki, S. Uchida, J. C. Davis, J. P. Sethna, and E.-A. Kim, *Nature (London)* **466**, 347 (2010).
- [22] D. Feinberg and J. Friedel, *J. Phys. (Paris)* **49**, 485 (1988).
- [23] S. Brazovskii and T. Nattermann, *Adv. Phys.* **53**, 177 (2004).